# Geomechanics Study of Ore and Host Rocks for Narrow Vein Mining

Yingjian Xiao, Stephen Butt
*Department of Process Engineering – Memorial University, St. John's, NL, Canada*

ABSTRACT
In Sustainable Mining by Drilling (SMD) method, mining excavation commonly transfers from open pit mining to drilling excavation based on the cost and efficiency. Mining drilling is generally conducted on narrow veins, along with next-step excavation using the hole-widening drilling. To obtain the maximum production, a comprehensive study is required for planning drill-off tests (DOT) aiming at the highest rate-of-penetration (ROP) or material-removal-rate (MRR). In Drilling Technology Laboratory (DTL), geomechanics parameters of ore and host rocks were obtained by a series of geomechanics tests. These parameters include peak strength, Young's modulus, acoustic properties, abrasiveness and hardness. Investigated rocks include argillite, altered mafic, high-pyrite mafic, ordinary mafic and quartzite. Core were drilled and compared from directions parallel and perpendicular to the bedding. In Pine Cove Deposit, high-pyrite mafic cores parallel to the beddings are stronger than that perpendicular to the beddings due to some existing quartz between beddings. In Romeo & Juliet Vein, mafic volcanic has much higher strength than that in Pine Cove Deposit. These geomechanics parameters assist in designing on-site DOT for the optimum production.

RÉSUMÉ
Dans la méthode d'exploitation durable par forage (SMD), l'excavation minière est généralement transférée d'une exploitation à ciel ouvert à une excavation de forage en fonction du coût et de l'efficacité. Le forage minier est généralement effectué sur des filons étroits, de même que l'excavation à l'étape suivante utilisant le forage d'élargissement du trou. Pour obtenir le maximum de production, une étude complète est nécessaire pour la planification d'essais de forage (DOT) visant le taux de pénétration le plus élevé (ROP) ou le taux d'enlèvement de matière (MRR). Dans le laboratoire de technologie de forage (DTL), les paramètres géomécaniques du minerai et des roches hôtes ont été obtenus par une série de tests géomécaniques. Ces paramètres incluent la résistance, le module de Young, les propriétés acoustiques, l'abrasivité et la dureté. Les roches étudiées comprennent l'argilite, le mafrique altéré, le mafique à haute teneur en pyrite, le mafique ordinaire et le quartzite. Les carottes ont été forées et comparées à partir de directions parallèle et perpendiculaire à la litière. Dans le gisement Pine Cove, les noyaux mafiques à haute teneur en pyrite parallèles à la stratification sont plus solides que ceux perpendiculaires à la stratification en raison de la présence de quartz entre les stratifications. Dans Romeo & Juliet Vein, le volcan mafic a une résistance bien supérieure à celle du gisement Pine Cove. Ces paramètres géomécaniques facilitent la conception de DOT sur site pour une production optimale.

## 1 INTRODUCTION

A Sustainable Mining by Drilling (SMD) method was proposed by the Drilling Technology Laboratory (DTL) at Memorial University of Newfoundland. This method of mining is distinctive from the conventional mining method, i.e. open pit mining. This SMD applies the standardized drilling methods and existing drilling apparatuses from oil and gas industry to exploiting veins in mining industry. This is specifically suitable for mining narrow veins where a large open pit is not necessary or not economic. Due to this, drilling related inputs have to be exclusively detailed, in particular the local geology.

This study reports a group of rock mechanics related parameters measured from multiple rocks in Anaconda Mining site, Baie Verte, Newfoundland and Labrador of Canada. These parameters were obtained by conducting standard geomechanical tests in DTL, where two newly developed instruments were employed. Those properties are essential for future rock penetration and fragmentation in SMD.

## 2 LITHOLOGY AND ROCKS

This section will give an introduction of the local geology at the mining site and rock collection. For the sake of research, a large variation of rock types are included to cover existing mining areas and potential excavation sites.

### 2.1 Geology

Figure 1 shows the local geology of the mining site (Copeland et al. 2015). It is mainly composed of the Pine Cove (PC) Deposit and the Romeo & Juliet (R&J) Vein.

The PC Deposit consists of several stacked mineralized lenses (e.g. Lightning Zone, Thunder Zone) in the hanging wall of the northward-dipping Scrape Thrust which locally was observed to have thin units of ultramafic and granitoid rocks. Although approximately parallel to the thrust, the mineralized zones at PC are also broadly stratabound within a northward dipping sequence of coarse and fine grained mafic rocks which contrast with highly cleaved amphibolitic rocks in the footwall of the thrust.

The Romeo and Juliet zones to the north of PC are different, however, in that they are thick quartz veins. The steep quartz veins at Romeo and Juliet attain thicknesses

of up to 4 meters. Angular, silicified wallrock fragments representing the adjacent metavolcanic rocks are common in the veins and tourmaline was noted locally. The veins themselves are enveloped by a significant halo of carbonate alteration and in places shallow dipping extensional veins were noted to merge with the main mass of a steeply dipping vein (Juliet South).

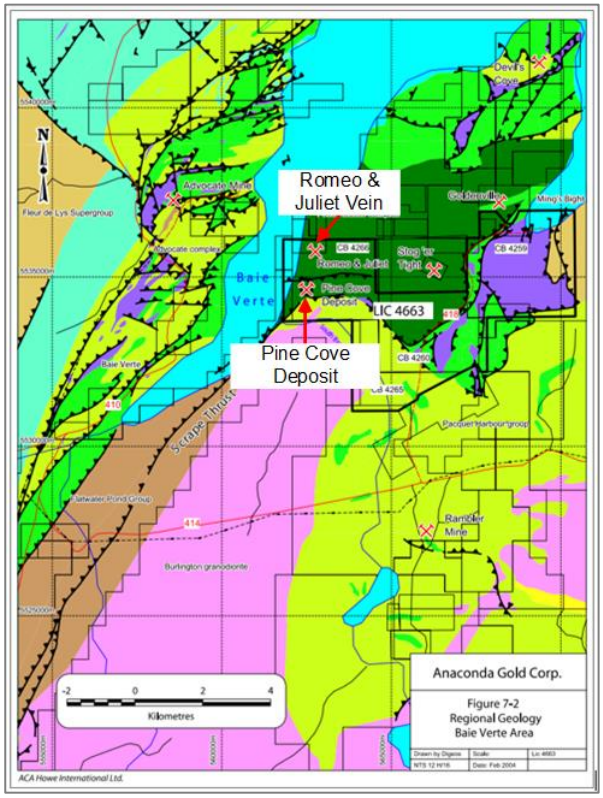


Figure 1. Map of Pine Cove Property in Baie Verte, Newfoundland, Canada. The red-cross hammers indicate Romeo & Juliet Vein and Pine Cove Deposit (courtesy of ACH Home International Ltd.)

## 2.2 Rock Samples

Four different types of rocks were selected in terms of accessibility and necessity for this study, i.e. mafic volcanic, altered mafic, argillite and quartzite. Figure 2 demonstrates the NQ standardardized size of samples, i.e. 47.6 mm in diameter, retrieved from the local core shack and by core drilling on outcrops (ASTM D4543−08, 2008). Gold exists in different rocks for the two mines. For example in the PC Deposit, the ore rock is mafic volcanic with a high content of pyrite. While in the R&J Vein, the ore rock is quartzite which is hosted by mafic volcanic. Here, both the high-pyrite mafic volcanic and quartzite are referred to be the ore rocks and other rocks are host rocks.

In summary, available cores for the PC Deposit are: high-pyrite mafic, mafic volcanic, altered mafic and argillite. Similarily, available cores for the R&J Vein are: quartzite and mafic volcanic.

## 3 EXPERIMENTS AND PROCEDURE

To obtain rock properties, testing apparatuses are provided in DTL and the Mechanical Lab at Memorial University. Table 1 assembles the testing parameters and corresponding apparatuses with the requirements of rock cores.

The parameters of strength include unconfined compression strength (UCS), confined compression strength (CCS) and point load index (PLI) strength which is supplementary to UCS and tensile strength. Non-destructive test (NDT) gives elastic wave velocities. Abrasiveness and hardness are essential for evaluating the bit wear and prediction of the bit life.

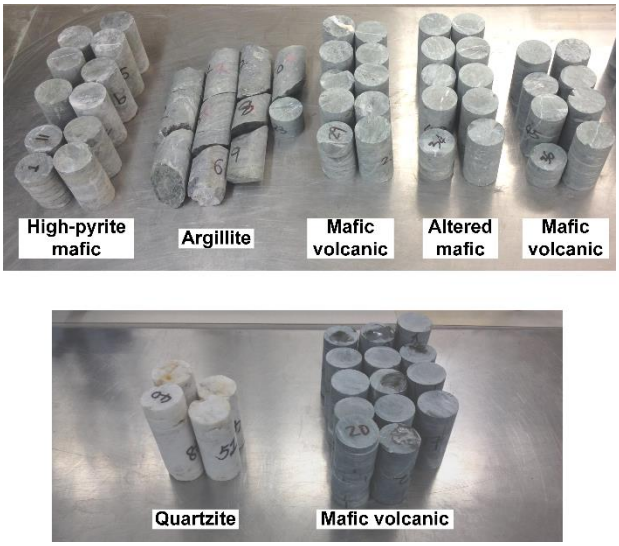


Figure 2. Assembly of core samples for PC Deposit (top) and R&J Vein (bottom). They are all in the size of NQ standard for the diameter

Table 1. Target experiments with preparation

| Test type | Parameters | Apparatuses | Sample |
|---|---|---|---|
| Strength | UCS, CCS strengths | Geomechanics frame | Core |
| | Young's modulus | Geomechanics frame | Core |
| | Tensile strength | Geomechanics frame | Disk |
| | PLI strength | PLI machine | Core |
| Non-destructive test | Acoustic elastic properties | NDT setup | Core or disk |
| Abrasiveness | CERCHAR abrasiveness | CERCHAR test machine | Core |

| | | | |
|---|---|---|---|
| Hardness | Hardness | Rebound hammer | Core |

### 3.1 Rock Strength Test

Conventional rock strengths, i.e. UCS and CCS, were measured directly on cores following a standard method from ASTM (ASTM D7012-10, 2010). It is worth noting that in DTL, a pressure servo machine was fabricated and put into use initially in this research, i.e. the geomechanics frame (Figure 3). This loading frame is distinctive to other commercial pressure servo apparatuses because of its manual operation. For example, it provides the advantage of conducting experiments which rigorously requires a static loading for a relatively long time such as creep test. Axial force was loaded by a vertical piston driven by hydraulic oil from a manually operated pump. The data acquisition (DAQ) software was developed based on the LabView platform. Both axial force and displacement were recorded and saved to computer disks automatically. The sampling rate was set to be 10 Hz for the current test, referring to other commercial universal testing machine.

During the UCS test, a core sample was placed between a load cell (sensor) and a loading piston with a steel platen for adjusting the core position. A minor axial force of approximate 0.1 kN was preloaded on the rock core before data collection. After the preload was set, data collection started and the axial force was increased by manually pushing pump. A transparent shield covered the sample for personnel protection. For the CCS test, a Hoek triaxial cell was connected to the geomechanics frame to provide a confining pressure which remained constant throughout the test. Now, a higher preload of approximate 2 kN was applied to sit the CCS test well.

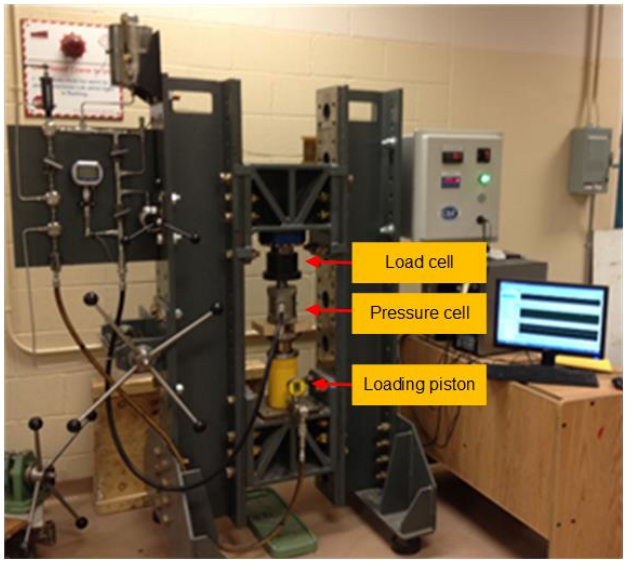


Figure 3. Demonstration of a CCS test under the new geomechanics frame at Memorial University

The splitting tensile strength was obtained from the indirect tensile strength test following a standard tensile strength method (ASTM D3967-08, 2008). Figure 4 demonstrated the splitting tensile test. The geomechanics frame was utilized to apply axial force on core disks. Core disks specimens were prepared following the standard that the ratio of core thickness and diameter ranged from 0.2 to 0.75. The axial force was applied incrementally and tensile failure generally occurred within 10 minutes.

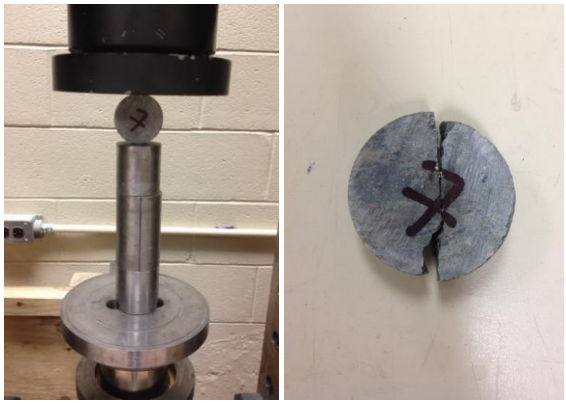

Figure 4. Demonstration of splitting tensile test (left) and tensile failure on the core disk (right)

For non-standard cores or irregular rocks that were not able to be cored, the PLI method was used to obtain the PLI strength as a supplementary option to the UCS (ASTM D5731−08, 2008). Figure 5 demonstrates a PLI test on a short core loaded between the two conical platens. This core was too short to meet the requirement of the UCS test. The load was steadily increased for a duration of 10 to 60 s until a maximum failure load was achieved. The failure pressure could be converted to the PLI strength based on the dimensions of rocks.

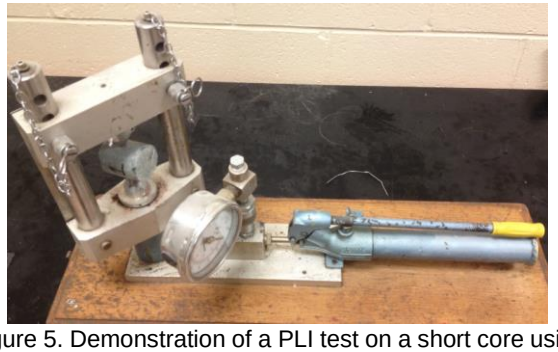

Figure 5. Demonstration of a PLI test on a short core using the PLI machine

### 3.2 Non-Destructive Test

The previous tests described were destructive and those rocks would not be reused any more. To solve this issue, a NDT method was applied to estimate rock related elastic

parameters, i.e. dynamic elastic parameters in contrast to those obtained from loading referred to be static elastic constants. Dynamic elastic constants were calculated from elastic wave (P and S) velocities measured from an NDT test (ASTM D2845-08, 2008). The test apparatus is demonstrated in Figure 6. Pulses with specific pulse repetition frequency (RPF) were initiated by a pulsar and transmitted through from a side of a rock core and received on the other side of this core. Both transmission and reception of the pulses were measured by two S-wave transducers, which are capable of transmitting and receiving both P and S waves. The pulses were altered when they travelled through the rock and received as irregular wavelets and displayed in an oscilloscope.

Due to the characteristic difference in P and S waves, P-wave travels faster than S-wave so that P-wave is always received earlier than S-wave. S-wave coexists with P-wave making it difficult to separate them. By rotating one of the two transducers (Figure 6), the first arrival of S-wave is recognized as the first polarization variation in waveforms during this rotation process. Both travel times are obtained by the reorganization of first arrivals of the two waves.

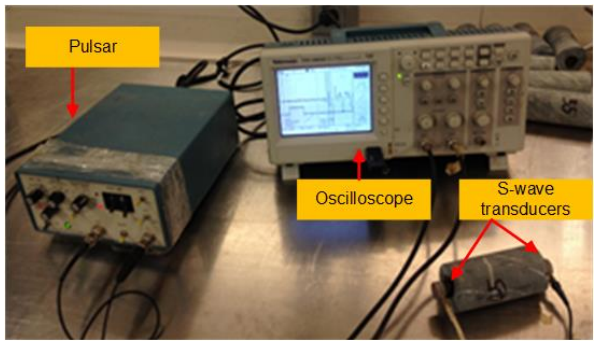

Figure 6. Demonstration of a NDT test

### 3.3 Abrasiveness

Abrasiveness is critical for bit wear and estimation of bit life. Rock abrasiveness was assessed by the CERCHAR abrasiveness method (ASTM D7625-10, 2010). The CERCHAR apparatus was demonstrated in Figure 7. Core samples were fixed vertically in the CERCHAR apparatus. A stylus was installed in steel mass which applied 70 N force axially on the stylus tip contacting rock surface. The hand lever pulled the steel mass along with stylus and the stylus tip moved horizontally to make a 10 mm scratch. Five parallel scratches on rock surface were then obtained.

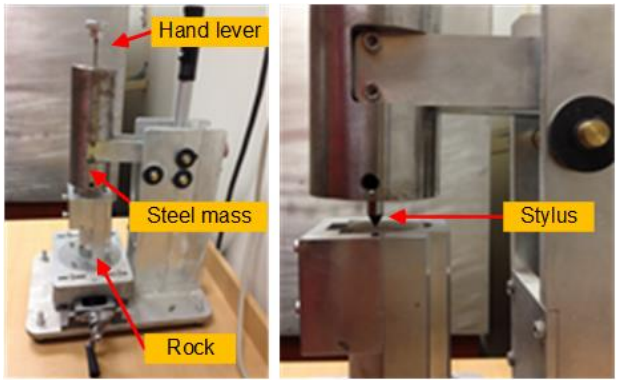

Figure 7. CERCHAR apparatus which is redesigned and fabricated at Memorial University

A microscope was then used to measure the scratch width as an indicator of the abrasiveness of the rock (Figure 8).

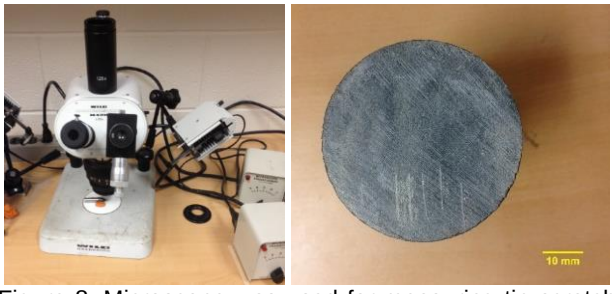

Figure 8. Microscope was used for measuring tip scratch width (left) of five straight lines left by a stylus (right)

### 3.4 Hardness

The hardness of rock was evaluated by a portable hammer, i.e. rebound hammer (ASTM D5873-14, 2014). A rebound number was obtained as an indication of rock hardness (Figure 9). When the hammer hit the rock surface, plastic and elastic deformations were generated on the rock surface. The hammer rebounded due to the relief of elastic deformation. During the test, a rock core was fixed and lay horizontally. The rebound hammber was put perpendicular to the rock core.


Figure 9. Hardness measurement by a rebound hammer

## 4 DATA PROCESSING AND RESULTS

This section will introduce the processing methods and procedures for data obtained from rock strength tests and non-destructive test. Parameters from tests and data processing will be assembled.

### 4.1 Data Processing

Figure 10 shows the raw data for a UCS test. Due to the data noise, smoothing was conducted on the data based on algorithms in Matlab. This smoothed curve was then referred to be the stress-strain curve. The maximum stress was identified as the UCS. The tangent slope of linear elastic portion was calculated and taken as the Young's modulus.

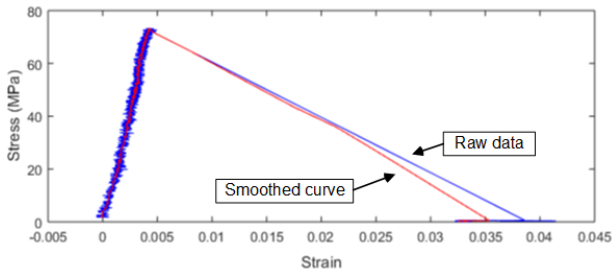


Figure 10. Discrete raw data for a UCS test with a smoothed stress-strain curve

For the PLI strength test, the PLI strength was estimated following Eq. 1 to Eq. 4.

$$S_{PLI} = k \times I_{s(50)} \quad [1]$$
$$I_{s(50)} = k \times I_s \quad [2]$$
$$F = (D/50)^{0.45} \quad [3]$$
$$I_s = P/D^2 \quad [4]$$

Where $S_{PLI}$ is the PLI strength, $I_{s(50)}$ is the index for the core with the diameter of 50 mm, F is the size correction factor with respect to the 50 mm diameter, P is the failure pressure, D is the diameter of the core, mm, K is the strength conversion factor retrieved from an empirical table.

Figure 11 shows the acoustic travel times for both P and S waves. Acoustic or dynamic elastic constants were then calculated based on rock density and acoustic travel velocities following Eq. 5 and Eq. 6.

$$E' = \left[\rho V_s^2\left(3V_p^2 - 4V_s^2\right)\right]/(V_p^2 - V_s^2) \quad [5]$$
$$\mu = (V_p^2 - 2V_s^2)/[2(V_p^2 - V_s^2)] \quad [6]$$

Where E' is the dynamic modulus, Pa, μ is the dynamic Poisson's ratio, $V_p$ and $V_s$ denote the measured P and S wave velocities, m/s, respectively. The two dynamic moduli are generally used to act as the elastic moduli if geomechanical tests are not possible to conduct (Fjaer et al. 2008).

### 4.2 Test Results from PC Deposit

This section provides resultant rock parameters for PC Deposit rocks. For every type of rock, previous tests were conducted to cover every aspect of rock parameters.

While, the dynamic moduli (E') are calculated from elastic wave velocities when the Young's moduli are not available. The dynamic Poisson's ratios (μ) are also calculated from these velocities when they are not able to be measured. They both can be used as a comparison of the static elastic moduli.

#### 4.2.1 High-Pyrite Mafic

Beddings were found in the high-pyrite mafic outcrops. To investigate the effect of beddings on rock properties, samples were cored along two directions, i.e. perpendicular and parallel to beddings. Table 2 and Table 3 list the geomechanics parameters, i.e. UCS, CCS, Young's modulus (E), CERCHAR abrasiveness index (CAI) and rebound hardness number R. Arithmetic average values are also obtained.

Average values were also taken for multiple other tests for dynamic modulus E', dynamic Poisson's ratio μ and tensile strength as 69.74 MPa, 0.12 and 10.13 MPa, respectively. It is shown that the dynamic modulus is significantly larger than the static Young's modulus. This agrees well with the past observations (Fjaer et al. 2008).

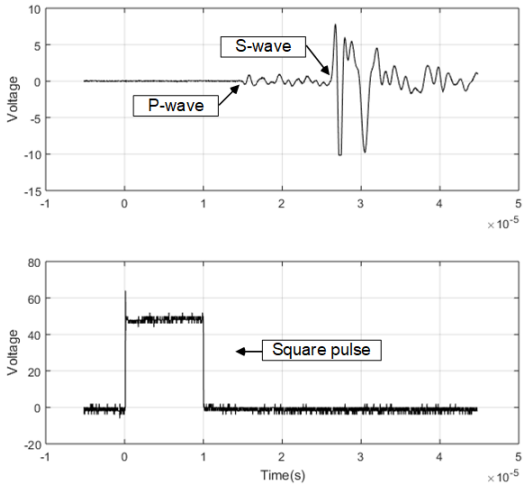


Figure 11. P and S waves are received and recognized as the first arrivals (top) and travel times are in reference to the start of transmitted square pulse (bottom)

Table 2. Geomechanics parameters for high-pyrite mafic samples cored perpendicular to beddings

| Core # | UCS (MPa) | CCS (@ 2 Mpa) | CCS (@4 Mpa) | E (GPa) | CAI (mm) | R |
|---|---|---|---|---|---|---|
| 1 | | | 97.71 | 10.62 | | 35 |
| 2 | 46.89 | | | 8.64 | | |
| 3 | | 91.24 | | 11.05 | | 35 |
| 8 | 31.90 | | | 11.60 | 0.63 | 29 |
| Average | 39.40 | 91.24 | 97.71 | 10.48 | 0.63 | 33 |

Table 3. Geomechanics parameters for high-pyrite mafic samples cored parallel to beddings

| Core # | UCS (MPa) | CCS (@ 2 Mpa) | CCS (@4 Mpa) | E (GPa) | CAI (mm) | R |
|---|---|---|---|---|---|---|
| 4 | | | 108.29 | 9.35 | | 34 |
| 5 | | 90.41 | | 16.10 | 0.69 | 31 |
| 6 | 68.60 | | | 16.69 | | 30 |
| 9 | 64.34 | | | 15.00 | | |
| Average | 66.47 | 90.41 | 108.29 | 14.29 | 0.69 | 32 |

### 4.2.2 Altered Mafic

Table 4 lists rock parameters for altered mafic based on the previous tests. An average of each parameter is provided.

For other parameters which are not demonstrated, average values were also taken from multiple other tests for dynamic modulus E', dynamic Poisson's ratio μ and tensile strength as 77.83 MPa, 0.24 and 10.05 MPa, respectively. This shows a significant larger value of dynamic modulus than Young's modulus (Fjaer et al. 2008).

Table 4. Geomechanics parameters for altered mafic

| Core # | UCS (MPa) | CCS (@ 2 Mpa) | CCS (@4 Mpa) | E (GPa) | CAI (mm) | R |
|---|---|---|---|---|---|---|
| 33 | | 88.75 | | 14.66 | | |
| 34 | | | 99.43 | 7.88 | | |
| 35 | 60.38 | | | 6.38 | | 37 |
| 37 | 40.99 | | | 9.76 | | |
| 38 | | | | | | 38 |
| 39 | | 97.82 | | 10.67 | | |
| 40 | | | 91.77 | 11.42 | 0.68 | 36 |
| Average | 50.69 | 93.28 | 95.60 | 10.13 | 0.68 | 37 |

### 4.2.3 Mafic Volcanic

Table 5 lists the geomechanics parameters from the ordinary mafic. An average of each parameter is provided.

For other parameters which are not demonstrated, average values were also taken for multiple other tests for dynamic modulus E', dynamic Poisson's ratio μ and tensile strength as 71.10 MPa, 0.20 and 10.54 MPa, respectively. This demonstrates a significant larger value of dynamic modulus than Young's modulus (Fjaer et al. 2008).

Table 5. Geomechanics parameters for mafic volcanic

| Core # | UCS (MPa) | CCS (@ 2 Mpa) | CCS (@4 Mpa) | E (GPa) | CAI (mm) | R |
|---|---|---|---|---|---|---|
| 26 | 59.24 | | | 9.35 | | |
| 27 | | | | | | 36 |
| 28 | | 71.93 | | 12.33 | | |
| 29 | 58.40 | | | 16.09 | | |
| 30 | 67.11 | | | 15.65 | | |
| 41 | | | | | | 40 |
| 42 | | 61.87 | | 8.31 | 0.67 | |
| 43 | 47.37 | | | 10.17 | | |
| 44 | 50.64 | | | 15.54 | | |
| 45 | | 71.09 | | 14.20 | | |
| 46 | | | | | | 39 |
| Average | 56.55 | 68.30 | | 12.70 | 0.67 | 38 |

#### 4.2.4 Argillite

Table 6 lists the geomechanics parameters from argillite. Splitting tensile strength test was done instead of standard strength test due to that cores were not accessible for standard strength tests.

Table 6. Geomechanics parameters for argillite

| Disk # | CAI (mm) | Elastic constants | | PLI (MPa) |
|---|---|---|---|---|
| | | E' (GPa) | μ | |
| 23 | 0.59 | 56.01 | 0.28 | 43.41 |

### 4.3 Test Results from R&J Vein

This section provides resultant rock parameters for R&J Vein rocks. For every type of rock, previous tests were conducted to cover every aspect of rock parameters. While, the dynamic moduli (E') are calculated from elastic wave velocities when the Young's moduli are not available. The dynamic Poisson's ratios (μ) are also calculated from these velocities when they are not able to be measured. They both can be used as a comparison of the static elastic moduli.

#### 4.3.1 Quartzite

Table 7 lists the geomechanics parameters for quartzite. An average of each parameter is provided.

For other parameters which are not demonstrated, average values were also taken for multiple other tests for dynamic modulus E', dynamic Poisson's ratio μ and tensile strength as 58.47 MPa, 0.13 and 8.50 MPa, respectively. Again, this shows a significant larger value of dynamic modulus than Young's modulus (Fjaer et al. 2008).

Table 7. Geomechanics parameters for quartzite

| Core # | UCS (MPa) | CCS (@ 2 Mpa) | CCS (@4 Mpa) | E (GPa) | CAI (mm) | R |
|---|---|---|---|---|---|---|
| 49 | 44.58 | | | 12.22 | | |
| 50 | | 52.03 | | 7.89 | 0.94 | |
| 51 | | | 88.89 | 10.05 | | 43 |
| Average | 44.58 | 52.03 | 88.89 | 10.05 | 0.94 | 43 |

#### 4.3.2 Mafic Volcanic

Table 8 lists the geomechanics parameters for mafic volcanic. An average of each parameter is provided.

For other parameters which are not demonstrated, average values were also taken for multiple other tests for dynamic modulus E', dynamic Poisson's ratio μ and tensile strength as 92.31 MPa, 0.25 and 21.54 MPa, respectively. This demonstrates a significant larger value of dynamic modulus than Young's modulus (Fjaer et al. 2008).

Table 8. Geomechanics parameters for mafic volcanic

| Core # | UCS (MPa) | CCS (@ 2 Mpa) | CCS (@4 Mpa) | E (GPa) | CAI (mm) | R |
|---|---|---|---|---|---|---|
| 10 | | | | | | 44 |
| 12 | | 116.39 | | 12.90 | | |
| 13 | | | | | | |
| 14 | | | 134.44 | 12.13 | | |
| 17 | 117.07 | | | 9.61 | | |
| 18 | 116.80 | | | 10.04 | | |
| 19 | | 114.15 | | 13.95 | | 47 |
| 20 | 73.21 | | | 21.06 | 0.76 | 47 |
| 21 | 68.07 | | | 15.60 | | |
| 22 | | | 133.52 | 12.10 | | |
| Average | 93.79 | 115.27 | 133.98 | 13.42 | 0.76 | 46 |

## 5 DISSCUSSION AND CONCLUSION

It is viable to obtain a detailed geomechanics parameters in laboratory which supports the future field mining operations and geotechnical studies.

The high-pyrite mafic has stronger strength parallel to the bedding than that in perpendicular direction due to some existing quartz between beddings. Mafic volcanic in R&J Vein has much higher strength than that in PC Deposit. This has been ignored before.

Dynamic elastic moduli are the other means of elastic moduli in addition to static moduli obtained by laboratory tests. The dynamic value has long been observed to be larger than the static value. This comes from the significant difference in strain amplitude due to plasticity or nonlinear effects.

A newly developed geomechanics loading machine is advantageous than other loading machine by the manual operation which is suitable for long-lasting tests.

Fractures are commonly found in rock cores which significant decrease the strength. Some fractures existing in outcrops which come from the excavation process. This may bias the results and outcrops will have to be selected considering this issue.

## 6 REFERENCES


ASTM D2845-08. 2008. Standard Test Method for Laboratory Determination of Pulse Velocities and Ultrasonic Elastic Constants of Rock. ASTM International, West Conshohocken, PA.

ASTM D3967-08. 2008. Standard Test Method for Splitting Tensile Strength of Intact Rock Core Specimens. ASTM International, West Conshohocken, PA.

ASTM D4543-08. 2008. Standard Practices for Preparing Rock Core as Cylindrical Test Specimens and Verifying Conformance to Dimensional and Shape Tolerances. ASTM International, West Conshohocken, PA.

ASTM D5731−08. 2008. Standard Test Method for Determination of the Point Load Strength Index of Rock and Application to Rock Strength Classifications. ASTM International, West Conshohocken, PA.

D5873-14. 2014. Standard Test Method for Determination of Rock Hardness by Rebound Hammer Method. ASTM International, West Conshohocken, PA.

D7625-10. 2010. Standard Test Method for Laboratory Determination of Abrasiveness of Rock Using the CERCHAR Method. ASTM International, West Conshohocken, PA.

ASTM D7012-10. 2010. Standard Test Method for Compressive Strength and Elastic Moduli of Intact Rock Core Specimens under Varying States of Stress and Temperatures. ASTM International, West Conshohocken, PA.

Copeland, D., Pitman, C., Evans, D., McNeill, P. and Slepcev, G. 2015. NI 43-101 Technical Report, Mineral Resource and Mineral Reserve Update on The Pine Cove Mine and Mineral Resource Estimate on The Stog'er Tight Deposit, Point Rousse Project. Anaconda Mining Inc. Technical Report.

Fjaer, E., Holt R.M., Horsrud, P., Raaen, A.M. and Risnes, R. 2008. *Petroleum Related Rock Mechanics*, 2nd ed., Elsevier B.V., Amsterdam, The Netherlands.